

Spectroscopy and Microscopy of Spin-Sensitive Rectification Current Induced by Microwave Radiation

Joonhee Lee,[†] Xiuwen Tu, and Wilson Ho*

Department of Physics and Astronomy and Department of Chemistry, University of California, Irvine, California 92697-4575

Received November 11, 2005

ABSTRACT

Amplitude-modulated microwave radiation was applied to the junction of a scanning tunneling microscope (STM). Rectification in the tunneling current was induced by the microwave because of the nonlinearity of the junction. It is shown that this rectification current is proportional to the d^2I/dV^2 signal and exhibits spin-sensitivity. The magnetic domain at the apex of an iron-coated tip was manipulated by applying an external magnetic field. The moment of spin flip and the magnetic hysteresis were measured by changes in the spin-dependent current through the Cr(001) surface.

Various extensions of scanning tunneling microscopy (STM) have been advanced to measure new physical quantities and interactions in addition to topography. The integration of microwave radiation and lasers with the STM has drawn much attention, in part to tap into the versatility of electromagnetic waves for excitation.¹ Rectification in tunneling current has been reported, arising from the nonlinear characteristics of the tunneling junction.^{2–8} The possibility of imaging insulators was proposed by laser irradiation of the tunneling junction,⁴ or applying a microwave signal to the tip,⁷ sample,⁸ or tip with sample mounted in a resonant cavity.⁹ Frequency mixing^{4–6} and photon-driven STM^{4,5} were also demonstrated by laser irradiation. In this paper, the microwave radiation is applied via a two-turn coil inserted in the STM junction, enabling nanoscale spectroscopy and microscopy. The induced rectification current could be measured by a novel approach of microwave modulation and used for probing nanoscale magnetism. Despite the macroscopic extent of the microwave radiation, antiferromagnetic domains at the nanometer scale could be resolved by spin-sensitive rectification current induced by a near-field microwave. The resolution of the magnetic domains led to the investigation of the magnetic properties of the thin film on the tip apex. The spin direction and the spin polarization of the sample were determined by recording the hysteresis curves of the tunneling current (I) versus the magnetic field (H). The stable junction tolerates the ramping magnetic field and enables novel $I-H$ measurement in the STM geometry.

* To whom correspondence should be addressed. E-mail: wilsonho@uci.edu.

[†] On leave of absence from Institute of Physics and Applied Physics, Yonsei University, Seoul 120-749, Republic of Korea.

The experiments were carried out at 18 K with a home-built STM with a base pressure of 2×10^{-11} Torr.¹⁰ A pair of external Helmholtz coils is used for supplying the dc magnetic field. The central axis of the coils is parallel to the sample surface plane. Nonmagnetic piezoelectric electrodes were used to suppress magnetostriction induced by the external magnetic field. The microwave radiation is supplied by two turns of the central conductor of a 50 Ω semirigid coaxial cable; the end of the cable is soldered to the ground shield of the cable. The Cr(001) surface was chosen to investigate the spin sensitivity of the rectification current induced by the microwave. This surface is known to exhibit alternating magnetization between adjacent terraces.¹¹ The Cr single-crystal surface was prepared by repeated cycles of Ne⁺ sputtering and annealing to 1013 K. W wires were electrochemically ac etched to form blunt tips compared to those obtained with ac followed by dc etchings. The flat apex of such blunt tips was found to be a better template for Fe film growth and the attainment of spin polarization electrons. The tips were flashed in vacuo by electron beam annealing to remove oxide, prior to coating with 20 monolayers of Fe by e-beam evaporation. The Fe-coated tips were annealed, followed by cooling in the presence of a 608 Oe magnetic field. The RF coil was positioned between the tip and the sample.

The microwave circuitry is illustrated in Figure 1a. In the present experiment, the circuit was tuned to 800 MHz, and the microwave was chopped at 200 Hz. A square wave modulation in tunneling current was observed, as shown in Figure 1b for 0.2 V rms microwave across the gap, arising from the coupling of microwave radiation's electric field to

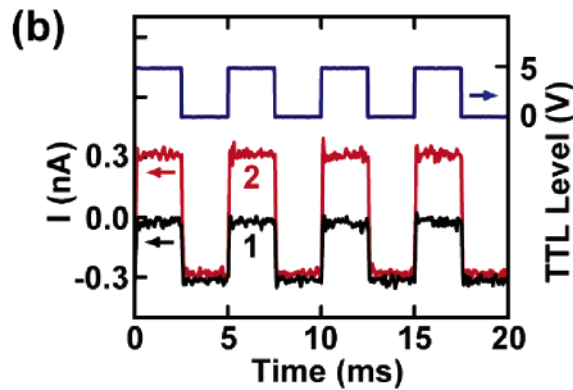
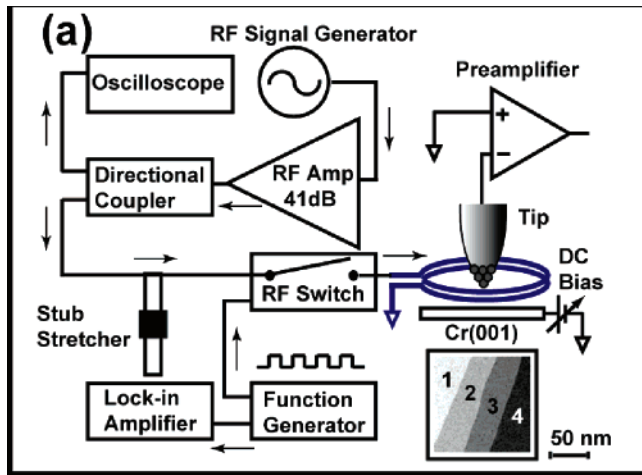


Figure 1. (a) Microwave circuit diagram. The amplified microwave is fed to a directional coupler; reflected power is monitored by the oscilloscope and minimized by adjusting the impedance matching with the stub stretcher. Transmitted radiation is amplitude-modulated by a TTL-driven RF switch at 200 Hz for rectification spectroscopy, and 3 kHz for microscopy. A two-turn RF coil is inserted between the tip and sample. (b) Modulated tunneling current vs time, showing different dc current enhancement during the presence of the microwave radiation. The TTL (top waveform) controls the RF switch; microwave radiation is transmitted to the coil when TTL is high (5 V) and is otherwise blocked. The bottom curves show the modulated tunneling current recorded over two adjacent terraces (labeled 1 and 2) on the Cr(001) surface. A relatively large rms amplitude of 0.2 V across the gap was used to clearly show the spin-sensitivity of the rectification current.

the junction.¹² If the tunneling current is expressed as a Taylor series expansion about the applied dc sample bias, V_B , then

$$I(V) = I_0(V_B) + \frac{dI}{dV} \Big|_{V_B} \sqrt{2} V_J \cos(\omega t) + \frac{d^2 I}{dV^2} \Big|_{V_B} V_J^2 \cos^2(\omega t) + (\text{higher order terms in } V_J) \quad (1)$$

where the total bias $V = V_B + \sqrt{2} V_J \cos(\omega t)$, $I_0(V_B)$ is the dc tunneling current at V_B , V_J is the rms amplitude of the induced voltage difference between the tip and the sample at the microwave frequency $\omega/2\pi$. Because the tunnel junction has nonlinear characteristics, multiple harmonics of microwave frequency are generated. However, because of the limited bandwidth of the current preamplifier (4 kHz at

10^9 V/A), the components of the current at ω and higher harmonics are averaged out by the preamplifier. Therefore, we consider only dc terms from eq 1

$$I_{dc}(V_B, V_J) = I_0(V_B) + I_R(V_B, V_J) = I_0(V_B) + \frac{1}{2} V_J^2 \frac{d^2 I}{dV^2} \Big|_{V_B} + (\text{higher order terms in } V_J) \quad (2)$$

where I_R is the dc rectification current.

To extract I_R from the larger I_0 , the microwave is chopped at low frequency ω_c . The rectification current, I_R , is similarly modulated and its time dependence is represented by

$$I(t) = I_0(V_B) + I_R \left(\frac{2}{\pi} \sum_{n=1,3,5,\dots}^{\infty} \frac{1}{n} \sin(n\omega_c t) + \frac{1}{2} \right) \quad (3)$$

where the expression in parentheses is the Fourier series of a square wave switching between 0 and 1. In Figure 1b, higher order derivatives in eq 2 are contained in the observed I_R because a large microwave amplitude was applied in order to visually display the rectification current signal. As illustrated in Figure 1b, the tunneling current is increased from -0.3 nA when the microwave irradiates the junction. This is due to the positive rectification current contribution at -32 mV bias on the Cr(001) surface. The difference in the rectification current on the two adjacent terraces reveals that it reflects the spin contrast because the Cr(001) surface has alternating magnetization between adjacent terraces. Because the rectification current excited by the microwave shows spin sensitivity with the spin-polarized tip, the antiferromagnetic character of Cr(001) can be spatially resolved by rectification microscopy.

A direct comparison between conventional scanning tunneling spectroscopy (STS) and microwave rectification spectroscopy (MRS) is shown in Figure 2. The $I(V_B)$ curves obtained in the presence (Figure 2a) and absence (Figure 2b) of the microwave show identical nonlinear characteristics of the tunneling junction. The density of state (DOS) spectrum, dI/dV , reveals the Cr surface state peak near the Fermi level.¹³ The MRS I_R spectrum¹⁴ in Figure 2c shows excellent agreement with the normal d^2I/dV^2 spectrum (Figure 2d). Even the small wiggles in the STS d^2I/dV^2 spectrum appear in the MRS I_R spectrum, demonstrating the dependence of the rectification current on d^2I/dV^2 , according to eq 2. This d^2I/dV^2 dependence was confirmed using the lock-in detection with controlled microwave coupling V_J ,¹² whereas the analyses of previous d^2I/dV^2 dependence of the rectification current by laser irradiation³⁻⁵ required numerical fitting.

Laser irradiation of the junction also led to photothermal modulation of the tunneling gap.¹⁵ To rule out gap modulation from microwave-induced thermal expansion, we performed $I-Z$ spectroscopy. The tunneling gap was modulated by 0.01 \AA at 200 Hz, and the first harmonic signal, dI/dZ , from the lock-in amplifier showed the same shape of curve as $I(V)$. This agreement is expected because the tunneling current, and, hence, dI/dZ , depend exponentially on gap

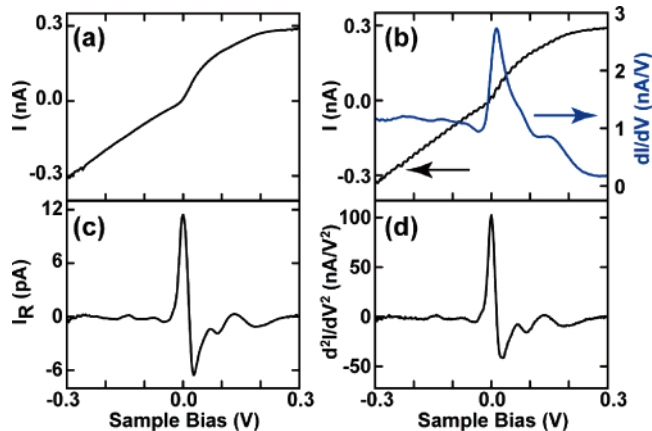


Figure 2. Comparison between microwave rectification spectroscopy (MRS) and conventional scanning tunneling spectroscopy (STS). Spectra were obtained from spatial average of eight individual spectra taken from terraces 1 and 3 of Figure 1a. dI/dV , d^2I/dV^2 , I_R spectra were acquired by lock-in technique. The tunneling gap was set at 0.3 nA, +0.3 V prior to opening the feedback loop. The sample bias was ramped in 2.5 mV step with 300 ms integration for each point. Each spectrum was averaged over six passes. The ac modulation of 10 mV rms was added to the sample bias for STS, and 10 mV rms microwave radiation (800 MHz) across the junction was modulated at 200 Hz for MRS (220 μ V rms from signal generator). (a) Tunneling current vs bias voltage (I - V curve) in the presence of modulated microwave radiation. (b) I - V curve from STS, and the simultaneously recorded dI/dV curve shows a prominent surface state peak. (c) Rectification current (I_R) spectrum, extracted from the tunneling current by recording the first harmonic signal in MRS. (d) d^2I/dV^2 spectrum by recording the second harmonic signal in STS.

distance. Therefore, we could exclude thermal effects in MRS because I_R differs clearly from an exponential function. This observation demonstrates the ability to extract a minute amount of current (<1 pA) induced by chopping the microwave without causing thermal effects; the current is doubly modulated at the RF and 200 Hz.

The spatial dependence of the rectification current leads to microwave rectification microscopy (MRM) that is complementary to dI/dV and d^2I/dV^2 scanning tunneling microscopy (STM). In Figure 3, four kinds of spatial images are shown: (a) constant current topography; (b) rectification current I_R ; (c) dI/dV ; and (d) d^2I/dV^2 . Each image was obtained at -32 mV sample bias. The antiferromagnetic order of the Cr(001) surface persists at 18 K, although spin density wave transition at 123 K was reported in the bulk.^{16,17} The contrast in the I_R image matches that in the d^2I/dV^2 image and shows opposite contrast from the dI/dV image. These results further confirm that I_R depends on d^2I/dV^2 and is spin sensitive. The I_R difference of 4 ± 6 pA between bright and dark terraces is calculated by averaging I_R values covering the dark (1, 3) terrace pair and bright (2, 4) pair. The large uncertainty arises from the inhomogeneity in the images, revealed as bright and dark features that are attributed to impurities and distribution of spin orientations inside each terrace. The spin contrast inversion between dI/dV and d^2I/dV^2 images is observed at -32 mV sample bias, and the same contrast is obtained at a larger sample bias of -150 mV.

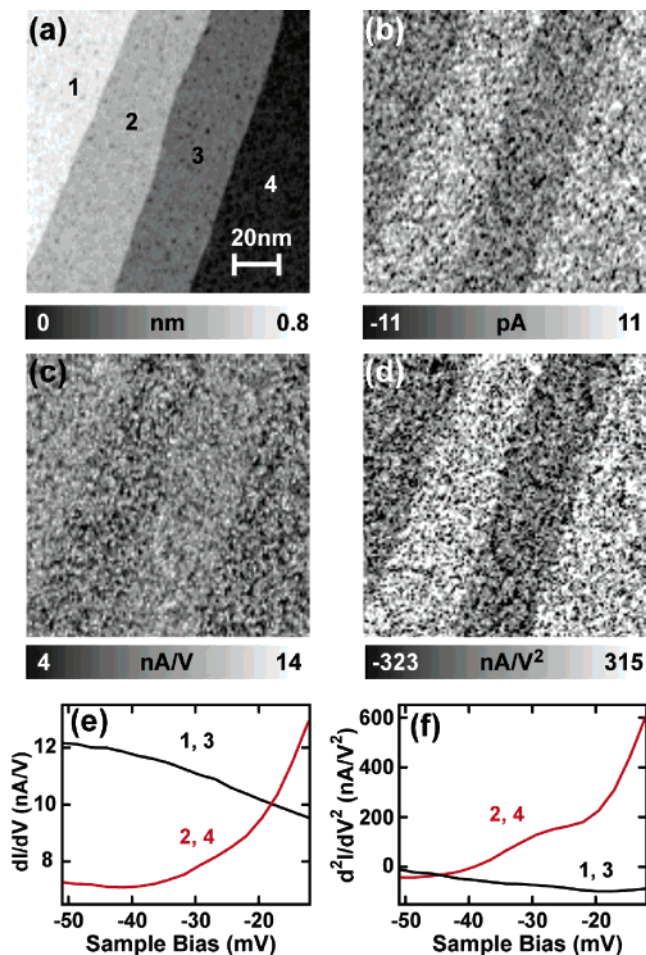


Figure 3. Comparison between dI/dV and d^2I/dV^2 scanning tunneling microscopy (STM) and microwave rectification microscopy (MRM). Images a, c, and d were obtained simultaneously, and b was acquired for the same area. A sample bias modulation of 10 mV rms amplitude and 1.5 kHz was used in STM with feedback on during microscopy. For MRM, 10 mV rms and 800 MHz microwave radiation across the gap was modulated at 3 kHz. The set point was 0.3 nA, -32 mV. (a) $2164 \text{ \AA} \times 2164 \text{ \AA}$ topography image. (b) I_R image. (c) dI/dV image. (d) d^2I/dV^2 image. (e) The (1, 3) terrace pair has a higher dI/dV signal than the (2, 4) pair at -32 mV, in agreement with dI/dV microscopy in c. (f) The (2, 4) terrace pair has a higher d^2I/dV^2 signal than the (1, 3) pair at -32 mV, consistent with the contrast inversion between dI/dV and d^2I/dV^2 signals.

The contrast reversal between different derivatives raises the necessity to determine the spin alignment configuration between the tip and sample. Tunneling current is monitored while maintaining a constant tunneling gap, with the feedback turned off, and ramping the dc magnetic field generated by a pair of external coils. This type of measurement is enabled by the stable junction in the presence of the magnetic field. A contrast reversal is observed to coincide with the flipping of the tip magnetization direction as shown in Figure 4. The spin-polarized tip was initially placed over the center of the image that was bright in the I_R image. As the magnetic field was ramped from 0 to -250 Oe after opening the feedback loop, an abrupt transition at -146 Oe was observed and none on the reverse ramping (Figure 4a). The I_R images recorded at the beginning and the end of the ramp revealed a contrast

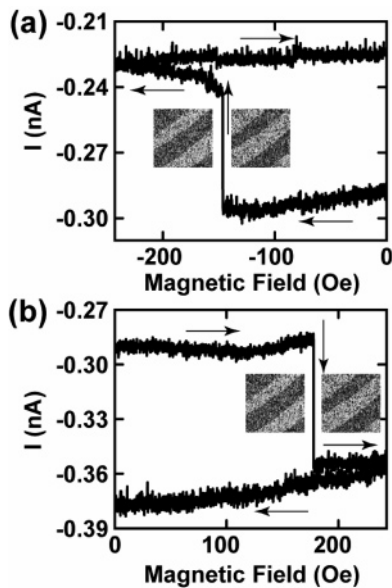


Figure 4. I (tunneling current) vs H (magnetic field) graph. The tunneling gap was set at 0.3 nA, -32 mV before opening the feedback loop, and the tunneling current was monitored during ramping of magnetic field from 0 to ± 240 Oe, in 0.16 Oe step and 300 ms read delay time. An additional 2-s delay was included when the magnetic field changes direction. The tip was placed over the center of the image. The magnetic field was first ramped from zero field to the maximum magnitude of 608 Oe and back to 0 Oe to impose tip spin orientation in the field direction (to set initial condition). Microwave rectification microscopy (MRM) was recorded before and after ramping of the magnetic field to check for spin flip of tip magnetization. The arrows show the direction of magnetic field ramp. (a) A step decrease in the magnitude of the current at -146 Oe was observed, and MRM shows contrast inversion. (b) A step increase in current magnitude at $+178$ Oe was observed, and the original spin contrast was recovered.

reversal. The antiferromagnetic order of the Cr surface cannot be reversed by these small external magnetic fields; thus, the spin of the tip apex must have been flipped. The original contrast could be recovered by reversing the direction of the magnetic field; the $I-H$ curve is plotted in Figure 4b. According to the spin valve effect,¹⁸ the magnitude of the current is increased (decreased) at the moment when the spin alignment of the tip relative to the sample changes from antiparallel (parallel) to the parallel (antiparallel) configuration. We can conclude that the bright terrace in the I_R image corresponds to parallel spin alignment configuration, and the dark terrace has the opposite configuration. To the best of our knowledge, these results represent the first measurement of the $I-H$ hysteresis curve by continuously varying the magnetic field in the STM geometry.

The Cr(001) surface polarization could be estimated from an effective polarization, P , given by eq 4,^{18,19} at a constant gap

$$P = P_{\text{Cr}} P_{\text{Fe}} = \frac{I_{\uparrow\uparrow} - I_{\uparrow\downarrow}}{I_{\uparrow\uparrow} + I_{\uparrow\downarrow}} \quad (4)$$

An effective polarization of the tunnel junction is estimated to be $9.2 \pm 1.3\%$, derived by averaging current changes from

seven independent $I-H$ curves. By adopting a thin Fe film polarization, P_{Fe} , of 44%,²⁰ the Cr(001) surface spin polarization, P_{Cr} , is deduced as $21 \pm 3\%$. This estimation agrees well with the result of $(18 \pm 2\%)$ from electron-capture spectroscopy.²¹ Measurement of the tunneling current at a constant gap and in a varying magnetic field facilitates the calculation of the spin polarization; otherwise, eq 4 is invalidated.²² This method of determination of spin polarization can be extended to other magnetic systems.

The tip apex is expected to consist of multiple Fe domains, and the avalanche of multiple magnetic domain movements can generate strain and heat. Magnetic domain change is known to be abrupt. Some spin-polarized tips resulted in multiple steps during both ramping directions of the magnetic field, and contrast reversal is rarely observed in these cases. In addition, after many spin flips, the tip becomes magnetically unstable, and the $I-H$ curve showed many steps and kinks, which can be interpreted as Barkhausen noise generation.²³ Even when the magnetic field resolution was increased 10-fold to 16 mG, the width of abrupt transitions as those in Figure 4 was not resolved. The abrupt transitions observed in Figure 4 are attributed to single magnetic domain change at the tip apex.

This paper presents a novel extension of the STM technique, involving its coupling to the RF electromagnetic radiation. The d^2I/dV^2 characteristics of the microwave-induced rectification current implies more than a trivial reproduction of the second derivative signal because it is achieved with microwave radiation. MRS and MRM can be applied to other scientific problems. For instance, the electric field component of microwave can be coupled to the molecular dipole and induce chemical transformation. The magnetic field component at microwave frequency can excite the local spin. The single spin excitation leads to a change in the rectification current associated with the microwave absorption in resonance with the Zeeman splitting in an external dc magnetic field. A sub-Kelvin temperature would be desirable for the measurement of such a small quantum of energy.

In summary, the application of a chopped microwave radiation into the STM tunneling junction gives rise to a dc rectification current. This rectification current is shown to depend on d^2I/dV^2 and exhibit spin sensitivity. The Cr(001) topological antiferromagnetism was observed with microwave rectification spectroscopy (MRS) and microscopy (MRM). The atomic-scale spin valve effect in the STM junction was observed by ramping an external magnetic field applied to the junction. The novel approach of measuring the spin-flip of the tip enabled the determination of its spin orientation.

Acknowledgment. This work was supported by the National Science Foundation Grant no. 0102887. J.H.L was additionally funded by the BK 21 project.

References

- (1) Wickramasinghe, H. K. In *Scanning Tunneling Microscopy*; Stroscio, J. A.; Kaiser, W. J.; Eds.; Academic Press: San Diego, CA, 1993.
- (2) Nguyen, H. Q.; Cutler, P. H.; Feuchtwang, T. E. *IEEE Trans. Electron Devices* **1989**, *36*, 2671.

- (3) Bragas, A. V.; Landi, S. M.; Martinez, O. E. *Appl. Phys. Lett.* **1998**, *72*, 2075.
- (4) Völcker, M.; Krieger, W.; Walther, H. *Phys. Rev. Lett.* **1991**, *66*, 1717.
- (5) Völcker, M.; Krieger, W.; Suzuki, T.; Walther, H. *J. Vac. Sci. Technol., B* **1991**, *9*, 541.
- (6) Krieger, W.; Suzuki, T.; Völcker, M.; Walther, H. *Phys. Rev. B* **1990**, *41*, R10229.
- (7) Bumm, L. A.; Weiss, P. S. *Rev. Sci. Instrum.* **1995**, *66*, 4140.
- (8) Kochanski, G. P. *Phys. Rev. Lett.* **1989**, *62*, 2285.
- (9) Seifert, W.; Gerner, E.; Stachel, M.; Dransfeld, K. *Ultramicroscopy* **1992**, *42*, 379.
- (10) The STM is a variation of the one described in the following: Stipe, B. C.; Rezaei, M. A.; Ho, W. *Rev. Sci. Instrum.* **1999**, *70*, 137.
- (11) Kleiber, M.; Bode, M.; Ravlic, R.; Wiesendanger, R. *Phys. Rev. Lett.* **2000**, *85*, 4606.
- (12) The coupling of the microwave to the STM was determined quantitatively from the Mn spectral splitting that is proportional to an effective potential developed across the tunnel junction.
- (13) Strosio, J. A.; Pierce, D. T.; Davies, A.; Celotta, R. J.; Weinert, M. *Phys. Rev. Lett.* **1995**, *75*, 2960.
- (14) The spectrum of microwave rectification current versus the sample bias is measured by calibrating the first harmonic signal from a lock-in amplifier. The microwave is amplitude modulated by a square wave, and the resulting rectified current can be decomposed into Fourier components. The first harmonic Fourier component is given by $X_1(t)_{\text{rms}} = I_R 2/\pi(1/\sqrt{2}) \sin(\omega_c t)$, as can be derived from eq 3. The amplitude of X_1 , and thus I_R , is obtained quantitatively from the lock-in amplifier and is in agreement with I_R obtained directly by measuring and extrapolating the difference in tunneling currents with microwave on versus off in the square wave modulation for larger microwave amplitudes (e.g., Figure 1b). This difference is too small and not resolvable for the microwave across the gap of $V_J = 10$ mV rms amplitude.
- (15) Amer, N. M.; Skumanich, A.; Ripple, D. *Appl. Phys. Lett.* **1986**, *49*, 137.
- (16) Berger, A.; Hopster, H. *Phys. Rev. Lett.* **1994**, *73*, 193.
- (17) Fawcett, E. *Rev. Mod. Phys.* **1988**, *60*, 209.
- (18) Slonczewski, J. C. *Phys. Rev. B* **1989**, *39*, 6995.
- (19) Wiesendanger, R.; Güntherodt, H.-J.; Güntherodt, G.; Gambino, R. J.; Ruf, R. *Phys. Rev. Lett.* **1990**, *65*, 247.
- (20) Tedrow, P. M.; Meservey, R. *Phys. Rev. B* **1973**, *7*, 318.
- (21) Rau, C.; Eichner, S. *Phys. Rev. Lett.* **1981**, *47*, 939.
- (22) Kubetzka, A.; Pietzsch, O.; Bode, M.; Wiesendanger, R. *Appl. Phys. A* **2003**, *76*, 873.
- (23) Feynman, R. P.; Leighton, R. B.; Sands, M. *The Feynman Lectures on Physics*; Addison-Wesley: New York, 1996; Vol. 2, pp 37–9.

NL0522330